Sixth International Symposium on Marine Propulsors
smp'19, Rome, Italy, May 2019

Experimental Study of Six-Component Forces on Surface Piercing Propeller in Uniform Flow

ZHOU Jian[1,2], LU Lin-zhang[1,2], RUI wei[1,2], ZHAI Shu-cheng[1,2]

[1]China Ship Scientific and Research Center (CSSRC), Wuxi, China
[2]Jiangsu Key Laboratory of Green Ship Technology, Wuxi, China

ABSTRACT

In order to consider the six-component forces of surface piercing propeller, which was load input provided for structural design of driving device, experimental study of six-component forces in uniform flow was conducted in deepwater towing tank. Firstly, the measurement balance was developed for measuring six-component forces. Secondly, Measuring and testing technology and data processing method was established. Model tests of six-component forces on surface piercing propeller under different immersions were also done and some favorable results were obtained, which show that great fluctuation in different directions. Especially the change of peak to peak should attract our attention. In semi immersion state, vertical and lateral forces account for more than 1/4 of axial thrust. Meanwhile important reference was also provided for designing surface piercing propeller of high speed craft.

Keywords

Experimental study, surface piercing propeller (SPP), 6-component, uniform flow

1 INTRODUCTION

Surface piercing propellers (SPP), also known as partially submerged propellers are recognized as an outstanding propulsion device for high-speed planing or semi-displacement craft. The SPP propulsion system includes driving unit and surface piercing propellers. Due to the blades entry and exit the free surface, it is a very complex unsteady problem. The hydrodynamic force has a direct influence over the structure design and its reliability. Meanwhile, the working conditions of the surface piercing propellers affect the navigation attitude of the craft and resistance performance. However, based on rational hydrodynamic theory, there are few reliable performance prediction methods. Young (2004) has done a lot of work based on potential method for the analysis of surface-piercing propeller flows. Ding E. B. (2007) investigated the effect of cupped section and performed the numerical simulations of the flow field of two sections entry free surface by using commercial RANS code Fluent. For SPP systems, many efficient experimental tests are done. Ferrando et al (1999&2006) carried out experimental tests and obtained the effect of many parameters (like immersion ratio, axial shaft slope, Weber number, pitch ratio) on the hydrodynamic of the SPP . Ding E. B. (2007) carried out the open water test of the series SPP with six blades in the depressurized towing tank. Olofsson N. (1996) measured the dynamic load on individual blade and obtained the influence of shaft yaw and inclination angles on the propeller characteristics at different Froude and cavitation numbers. Pustoshny et (2007) presented the results of the development of 5-blades SPP series for fast speed boats. In this paper, experimental study of six-component forces on surface piercing propellers in uniform flow is conducted.

2 TEST MODEL

The test model has a diameter of 0.245m and 6 blades. The anodic oxidation was done on the surface of the SPP model. Before test the machining accuracy was checked again. Table 1 gives the main parameters of SPP model. Figure 1 gives the photo of SPP model with a number of TM17182A.

Table 1 Main parameters of SPP model

Model NO.	TM17182A
Diameter(D)	245.00mm
No. of blade (Z)	6
Expanded area ratio (Ae/Ao)	0.8
（P/D）$_{0.7R}$	1.57
Hub-Diameter ratio(d_h/D)	0.155
Rotation (viewing at downstream)	Right hand
Material	AL12

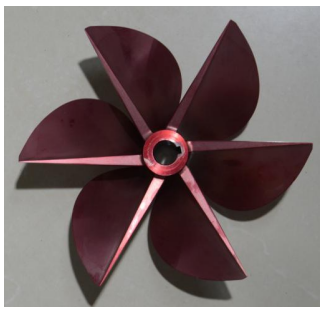

Figure 1 Model photo of SPP

3 EXPRIMENTAL SETUP AND METHOD

Hydrodynamic testing was conducted in the deepwater towing tank of CSSRC, The tank has dimensions of 474 m length by 7m depth by 14 m width, and the carriage is capable of speeds up to 10 m/s. The photo of the deepwater towing tank is showed in Figure 2. The dynamometer of six-component forces was installed under the carriage. During the model setup, the SPP model was drove by extension end of the dynamometer. The fore of the dynamometer was fixed by a guide cap and downstream part was used in the middle of the dynamometer. The whole experimental device consists of SPP model, multi-component of forces measurement system, revolution driving motor and revolution measurement device.

Figure 2 The photo of the deepwater towing tank

The depth of immersion of the SPP is shown in Figure 3. The immersion ratio (i) is h/D, where D is the diameter of the SPP and h is the depth of the lowest blade tip under water surface. Different immersion ratios are achieved by moving the carriage up and down.

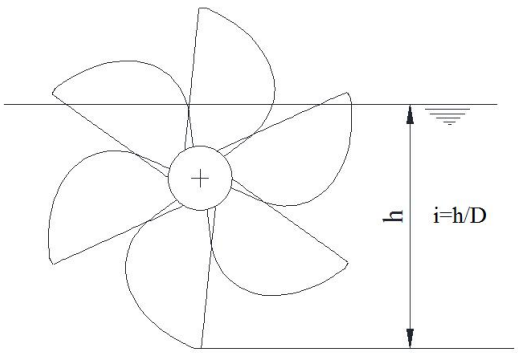

Figure 3 Depth of immersion (h) of the SPP

Model setup and data acquisition systems are shown in Figure 4. The six-component force balance with a rod type is shown in Figure 5.

Figure 4 Model setup and data acquisition system

Figure 5 Balance of six-component force

During the testing, both force and moment of axial direction, side direction and vertical direction should be measured. The phase value also should be recorded to concern the relationship between time and six-component forces. Changing the inflow velocity (V) and keeping the revolution (n) invariable were done and different velocities are controlled by carriage speed. Experimental method follows:

1) Measure the distance (L) between the center of propeller plane (O') and the calibration center of balance (O) after fixing the SPP model.

2) Adjust the vertical location of the dynamometer (carriage) to set the immersion ratio (i) to the test position.

3) Record the output signal of six-component forces and the dynamometer encoder (sampling frequency=5000Hz), when n=0.5 s^{-1} and v=0m/s.

4) Record the output signal of six-component forces and the dynamometer encoder (sampling frequency=80000 Hz), when n = n_{test} s^{-1} and V = V_{test} m/s.

The tests of different immersion ratios and advance coefficients are carried out for TM17182A. To measure the forces of low advance coefficients, the inflow velocity can't meet the requirement of the Froude number of velocity. So according to the requirement of the Froude number of revolution, the test revolution is confirmed in the tests. Table 2 gives the details of the test conditions.

Table 2 Test conditions

Model NO.	immersion ratio(i)	advance coefficient(J)	revolution (n)
TM17182A	0.3,0.5,0.7,0.9	0,0.50,0.75, 1.00,1.35	20 s^{-1}

4 RESULTS AND DISCUSSION

4.1 Method of test data processing

Generally speaking, the forces of the propeller plane are more concerned in the process of designing and analysis. However, the shaft of the model propeller is too small that the balance often can't be placed in the propeller plane and the result can't be got directly. The balance should be fixed in larger space and rotates together with the propeller shaft during test. So three coordinate systems including rotating coordinate system(o-xyz), fixed coordinate system(O-XYZ) and fixed coordinate system(O'-X'Y'Z') are required for helping data processing. Coordinate definition and data processing method are followed:

1) Coordinate definition

Both the origins of coordinate of the rotating coordinate system (o-xyz), and the fixed coordinate system (O-XYZ) are the calibration center of balance. The ox-axis and OX-axis coincide with propeller shaft. The inflow direction is positive. The rotating coordinate system (o-xyz) rotates with the SPP model. In the fixed coordinate system (O-XYZ), the OZ-axis represents the direction of the vertical force, which up is positive. The OY-axis represents the direction of side force, which satisfying the right-hand rule with the OZ-axis. Along the opposite direction of inflow, translate the fixed coordinate system (O-XYZ) a distance (L) to the center of propeller plane (O'), the fixed coordinate system (O'-X'Y'Z') is created. In the test, L=0.106m. The three coordinate systems are shown in Figure 6 and Figure 7.

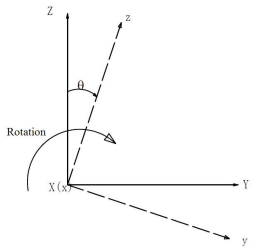

Figure 6 Rotating coordinate system (o-xyz), fixed coordinate system (O-XYZ) and rotation

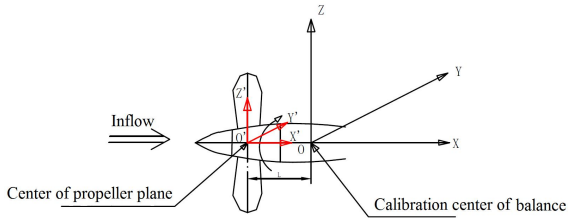

Figure 7 Fixed coordinate system (O-XYZ) and (O'-X'Y'Z')

2) Data processing

(a) Hydrodynamic calculation in rotating coordinate system (o-xyz)

Equation (1) gives the hydrodynamic calculation method in rotating coordinate system (o-xyz).

$$F_i = C_i^i \Delta V_i + \sum_{\substack{j=1 \\ j\neq i}}^{6} C_i^j F_j + \sum_{j=1}^{6}\sum_{l=j}^{6} D_i^{jl} F_j F_l \qquad (i,j = 1,2,...,6) \qquad (1)$$

Where C and D are the balance calibration coefficient; ΔV = output voltage minus zero voltage.

(b) Hydrodynamic calculation in fix coordinate system (O-XYZ) and (O'-X'Y'Z')

After getting the hydrodynamic results in rotating coordinate system (o-xyz), hydrodynamic calculations in fix coordinate system (O-XYZ) can be obtained by using Equation (2) and hydrodynamic calculations in fix coordinate system (O'-X'Y'Z') can be obtained by using Equation (3).

$$\begin{bmatrix} F_X \\ F_Y \\ F_Z \\ M_X \\ M_Y \\ M_Z \end{bmatrix} = \begin{bmatrix} 1 & 0 & 0 & 0 & 0 & 0 \\ 0 & \cos\theta & \sin\theta & 0 & 0 & 0 \\ 0 & -\sin\theta & \cos\theta & 0 & 0 & 0 \\ 0 & 0 & 0 & 1 & 0 & 0 \\ 0 & 0 & 0 & 0 & \cos\theta & \sin\theta \\ 0 & 0 & 0 & 0 & -\sin\theta & \cos\theta \end{bmatrix} \cdot \begin{bmatrix} F_x \\ F_y \\ F_z \\ M_x \\ M_y \\ M_z \end{bmatrix} \qquad (2)$$

Where F_X, F_Y, F_Z, M_X, M_Y and M_Z are results in fix coordinate system (O-XYZ); F_x, F_y, F_z, M_x, M_y and M_z are results in rotating coordinate system(o-xyz); θ = included angle between oz-axis and OZ-axis, its forward direction is consistent with rotation of the SPP model.

$$\begin{bmatrix} F'_X \\ F'_Y \\ F'_Z \\ M'_X \\ M'_Y \\ M'_Z \end{bmatrix} = \begin{bmatrix} 1 & 0 & 0 & 0 & 0 & 0 \\ 0 & 1 & 0 & 0 & 0 & 0 \\ 0 & 0 & 1 & 0 & 0 & 0 \\ 0 & 0 & 0 & 1 & 0 & 0 \\ 0 & 0 & -L & 0 & 1 & 0 \\ 0 & L & 0 & 0 & 0 & 1 \end{bmatrix} \cdot \begin{bmatrix} F_X \\ F_Y \\ F_Z \\ M_X \\ M_Y \\ M_Z \end{bmatrix} \qquad (3)$$

Where F'_X, F'_Y, F'_Z, M'_X, M'_Y and M'_Z are results in fix coordinate system (O'-X'Y'Z') ; L is the distance between the center of propeller plane (O') and the calibration center of balance (O).

(c) Dimensionless processing

Dimensionless processing of the 6-component forces in fixed coordinate system (O'-X'Y'Z') is shown in Equation (4).

$$\begin{aligned} [KTx, KTy, KTz] &= [F'_X, F'_Y, F'_Z] / \rho n^2 D^4 \\ [KMx, KMy, KMz] &= [M'_X, M'_Y, M'_Z] / \rho n^2 D^5 \end{aligned} \qquad (4)$$

4.2 Analysis of results

The tests are carried out for TM17182A with different immersion ratios including i=0.3, 0.5, 0.7 and 0.9. The test photo in some condition is shown in Figure 8.

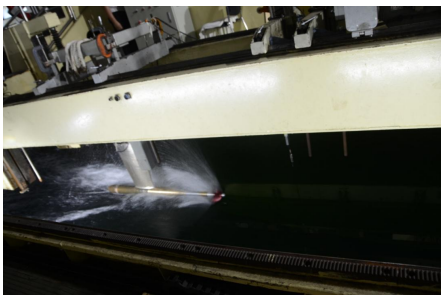

Figure 8 Test photo in some condition

After data processing, six-component forces of the center of the propeller plane are obtained, whose results are in the fix coordinate system (O'-X'Y'Z'). Different fluctuation curves of 6-component forces in fix coordinate system (O'-X'Y'Z') in the design advance coefficient J=1.35 are shown in Figure 9.

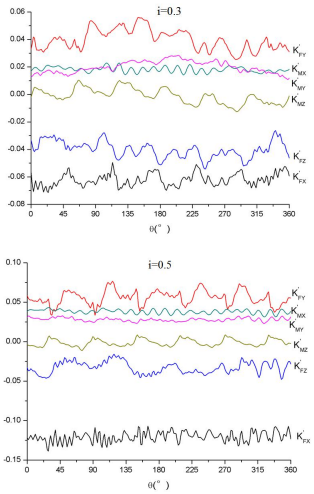

Figure 9 Different fluctuation curves of 6-component forces in fix coordinate system (O'-X'Y'Z') (J=1.35)

Figure 9 shows the fluctuation of force and moment in different directions over time in immersion ratio i=0.3 and i=0.5. The force direction of the vertical force is down and the force direction of the side force is pointing to the right side over the right hand SPP. The peak to peak value shows great fluctuation in different directions.

The average value results in different immersion ratios by Fourier analysis are shown in Figure 10. Figure 11 gives both the proportion of vertical average force and side average force to axial average force and the proportion of vertical average moment and side average moment to axial average moment. Change of 6-component forces and coordinate position of force point with different immersion ratios in design advance coefficient J=1.35 are shown in Figure 12 and Figure 13 separately.

In Figure 10, the change rule of the axial average force coefficient (KTx) and axial average moment coefficient (KMx) with the change of the advance coefficient J keep pace in immersion ratio i=0.3 with other immersion ratios. With the increase of the immersion ratio, the absolute values of the axial average force coefficient (KTx) and axial average moment coefficient (KMx) are increase also in the same advance coefficient. However, the change rules of KTy, KMy, KTz and KMz are worse than KTx and KMx, especially with the decrease of immersion ratios.

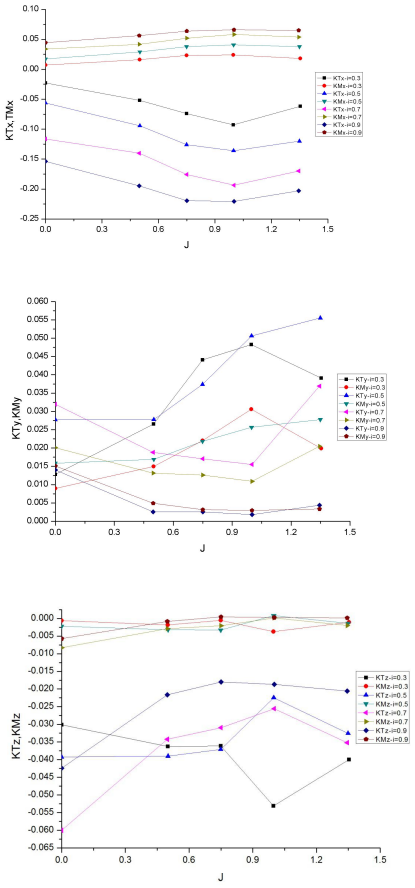

Figure 10 The average value results in different immersion ratios

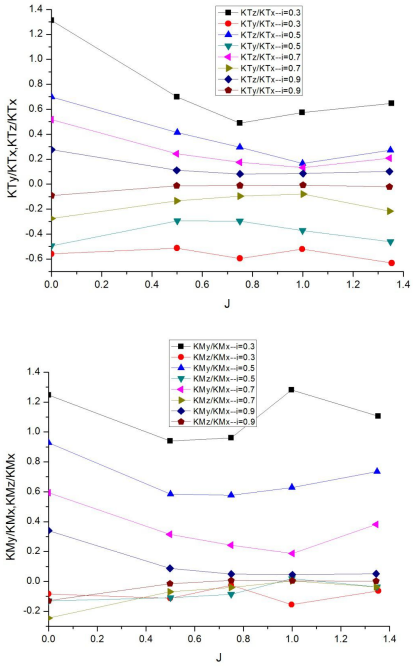

Figure 11 KTy/KTx, KTz/KTx, KMy/KMx and KMz/KMx curves

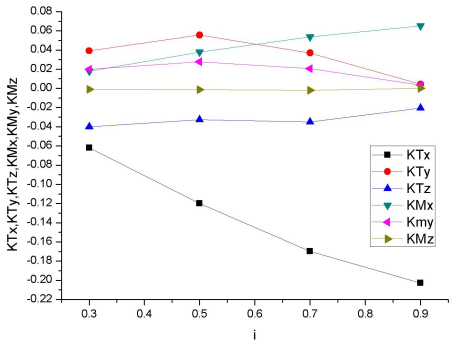

Figure 12 Change of 6-component forces with different immersion ratios(J=1.35)

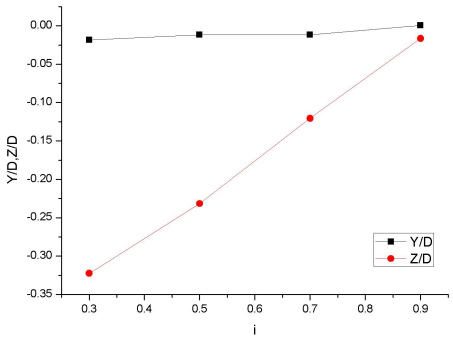

Figure 13 Change of coordinate position of force point with different immersion ratios(J=1.35)

Compared with KTx and KMx, the absolute values of KTy, KMy, KTz and KMz are smaller and their change rules are not easy to judge. So based on the KTx and KMx separately, KTy/KTx, KMy/KMx, KTz/KTx and KMz/KMx are obtained in Figure 11. With increase of the advance coefficient, most of KTy/KTx KTz/KTx are decrease first and then increase in the same immersion ratio. With increase of the immersion ratio, KTy/KTx KTz/KTx are decrease in the same advance coefficient and the change rule of KTy/KTx KTz/KTx with the increase of J tends to stabilize. KMy/KMx and KMz/KMx have similar change rule with KTy/KTx KTz/KTx in most advance coefficients. In immersion ratio i=0.9, KTz/KTx(vertical force) is larger than KTy/KTx(side force), the trend has weakened with the immersion ratio increasing especially in higher J. In design advance coefficient J=1.35, both the absolute values of KTz/KTx and KTy/KTx exceed 25% when the immersion ratio i less than 0.5. KMy/KMx are larger than KMz/KMx.

From Figure 12 and Figure 13, in design advance coefficient J=1.35, KTx and KMx are keeping decrease with the decrease of the immersion ratio. KTy and KTz are increase first and then decrease with the decrease of the immersion ratio and reach the maximum in i=0.5. The coordinate position of force point gradually moves to the center of the propeller plane with increase of the immersion ratio.

5 CONCLUDING REMARKS

Model tests of six-component forces on surface piercing propeller under different immersions were carried out and some favorable results were obtained. From the results presented in this study the following main conclusions can be drawn:

The peak to peak value shows great fluctuation in different directions. The force direction of the vertical force is down and the force direction of the side force is pointing to the right side over the right hand SPP. External rotation arrangement of the double SPPs is easier for the design of the connecting rod between the SPPs.

Side force and vertical force are increase first and then decrease with the decrease of the immersion ratio and reach the maximum in i=0.5. In semi immersion state, vertical and lateral forces account for more than 1/4 of axial thrust. The coordinate position of force point gradually moves to the center of the propeller plane with increase of the immersion ratio. The navigation attitude and resistance performance of the craft affected by the working condition of the surface piercing propellers should be considered during designing the SPP.

REFERENCES

Olofsson N. (1996) . 'Force and flow characteristics of partially submerged propeller', Doctoral Thesis, Goteborg: Chalmers University of Technology – Department of Naval Architecture and Ocean Engineering, Sweden.

Ding E. B. (2007). 'A series of surface piercing propellers and its application', Ninth International Conference on Fast Sea Transportation FAST2007, Shanghai, China.

Ferrando M., Scamardella A (1999). 'Surface piercing propellers: model tests procedures and comments on related dimensional parameters', Proceedings 5th Symposium on High Speed Marine Vehicles, Capri.

Ferrando M., Viviani M., Crotti S., Cassella P., Caldarella S.(2006). 'Influence of Weber number on surface piercing propellers model tests scaling', Proceedings of 7th International Conference on Hydrodynamics (ICHD), Ischia.

Young, Y.L. (2004). 'A simple hydroelastic model for surface piercing propellers', Proc. 25th Symp. on Naval Hydrodynamics, St. John's, Canada.

Pustoshny, A.V., Bointsov, V., Lebedev, E.P., Stroganov, A.A. (2007). ' Development of 5-blade SPP series for fast speed boat', FAST2007, Shanghai, China.